Quantum interface to charged particles in a vacuum

Hiroshi Okamoto*
Department of Electronics and Information Systems, Akita Prefectural University, Yurihonjo 015-0055, Japan
(Received 2 June 2014; published 3 November 2015)

A superconducting qubit device suitable for interacting with a flying electron has recently been proposed [Okamoto and Nagatani, Appl. Phys. Lett. **104**, 062604 (2014)]. Either a clockwise or counterclockwise directed loop of half magnetic flux quantum encodes a qubit, which naturally interacts with any single charged particle with arbitrary kinetic energy. Here, the device's properties, sources of errors, and possible applications are studied in detail. In particular, applications include detection of a charged particle essentially without applying a classical force to it. Furthermore, quantum states can be transferred between an array of the proposed devices and the charged particle.

DOI: 10.1103/PhysRevA.92.053805 PACS number(s): 37.20.+j, 42.30.−d, 07.77.Ka, 07.78.+s

I. INTRODUCTION

Quantum information processing methods may involve both the flying qubits and fixed qubits. One example is the quantum repeater [1], where fixed qubits could be used to realize long-distance quantum communication based on flying photons. Distributed quantum computing is another example, which would also employ photons as flying qubits connecting different parts of the computer [2,3].

Flying *electrons*, combined with fixed superconducting qubits [4], could also perform useful tasks. A known possible application of such a scheme is entanglement-assisted electron microscopy [5,6] for radiation sensitive biological specimens [7]. The use of a superconducting charge qubit [5] and a radio frequency superconducting quantum interference device (rf-SQUID) qubit [6] has been suggested to reduce the noise level down to the Heisenberg limit.

In what follows, we will focus on the rf-SQUID qubit rather than the charge qubit because generally a magnetic qubit appears to be more convenient in practice, especially when high energy charged particles are used. In particular, we will find that the rf-SQUID qubit, or a variant of it, allows us to detect single-charged particles while applying an exponentially small classical force to them, or in other words, essentially without applying a force on them. (The precise meaning of "exponentially small" will be explained in Sec. III D.) Charged particle detection with such a property could be useful in various relevant fields such as particle physics. More generally, we will show that bidirectional quantum information transfer between a single-charged particle and an array of qubits are possible in principle, opening ways to a wider range of applications.

The paper is organized as follows. Section II reviews the rf-SQUID qubit designed for our purpose. We then present how the single-charged particle detection works with our device. In Sec. III we consider in detail various sources of charged particle detection errors. In Sec. IV, after brief discussion of the operation sequence, we first discuss a possible application of the charged particle detector in biology. Second, to illustrate another more distant yet fundamentally sound possibility, we extend our single-qubit scheme to a multiqubit scheme to enable bidirectional quantum information transfer between a charged particle and a superconducting quantum information processor. Section V concludes the paper.

We note the recent proposal on the use of *trapped* electrons with superconducting qubits [8]. We assume that degrees of freedom other than the center-of-mass position of the charged particle, such as the spin degree of the electron, is well isolated in our scheme and ignore such extra degrees of freedom in this paper. The symbol "e" denotes the positron charge. We use the SI system of units as opposed to the Gaussian system throughout the paper, particularly with regard to definitions of electromagnetic quantities.

II. MAIN SCHEME

The structure of our rf-SQUID is schematically illustrated in Fig. 1(a). Whereas the standard rf-SQUID traps a magnetic flux in a superconducting ring interrupted by a Josephson junction, the rf-SQUID we analyze in this paper comprises a superconducting *tube that in turn makes a ring* and an associated Josephson junction [6]. The trapped magnetic flux in our case resides in the tube and, consequently, has the shape of a closed curve. In the particular case of Fig. 1, the tube has a long rectangular cross section and has a narrow, circular slit on the outer surface. The slit is bridged by a Josephson junction, making the device equivalent to the standard rf-SQUID in terms of electrical circuit topology. Although perhaps this is about the worst possible SQUID magnetometer design, we will show that the design could offer some uses in charged particle optics when the rf-SQUID acts as a qubit [9]. Henceforth, the term "rf-SQUID" refers to the type of device just mentioned unless stated otherwise. The main reason that the rf-SQUID device has some uses despite the confined magnetic flux is because the charged particle "feels" the magnetic flux via the Aharonov-Bohm (AB) effect [10].

We briefly review how a charged particle interacts with the rf-SQUID. Recall that the standard rf-SQUID qubit needs to be pierced by an external magnetic flux $\phi_0/2$, where $\phi_0 = h/2e$ is the magnetic flux quantum. (The circuitry to produce such a flux bias is not shown in Fig. 1.) This goes against the natural tendency of any superconducting ring to make the trapped magnetic flux an integer multiple of ϕ_0. Consequently, two equally energetically favorable states, with the trapped magnetic flux close to 0 or ϕ_0, respectively, are produced.

*okamoto@akita-pu.ac.jp

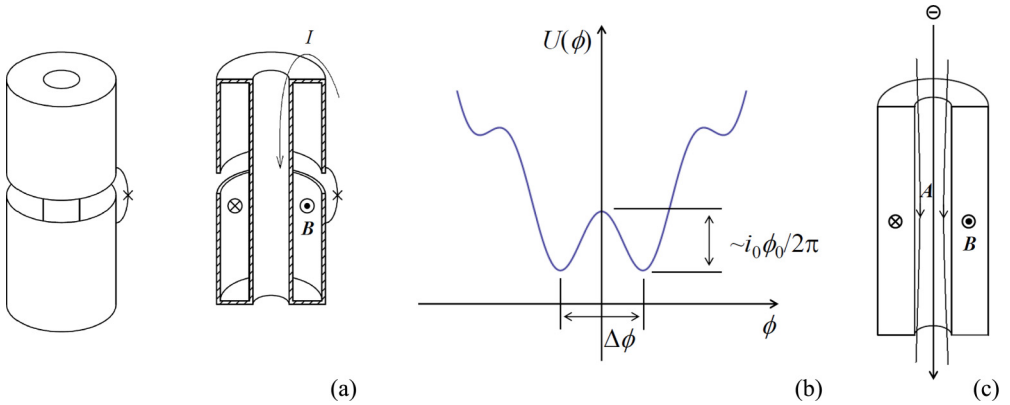

FIG. 1. (Color online) rf-SQUID qubit. (a) The overall structure. A cross section is shown on the right. The persistent current I, as shown by the arrow, flows through a double-walled tube, i.e., a hollow ring, with a slit on the outer surface. A Josephson junction ("X" symbol) is inserted across the slit. A ring-shaped magnetic flux (only $\otimes$, $\odot$ symbols are shown) is trapped inside the hollow ring (right). This particular state of the flux represents the state $|0\rangle_q$. (b) The potential energy landscape of an rf-SQUID that is biased with an external magnetic flux $\phi_0/2$. The graph is plotted as a function of the trapped magnetic flux in the rf-SQUID. (c) A negatively single-charged particle such as the electron, represented by a circle with a negative sign, follows the flow of the $\boldsymbol{A}$ field. As in (a), the $\boldsymbol{B}$ field corresponds to the state $|0\rangle_q$.

In the scheme presented in Ref. [6], the magnetic flux ϕ is within the tube, while the external bias flux $\phi_0/2$ is applied in a separate part of the device. This leads the tube to contain a magnetic flux of approximately either $\phi_0/2$ or $-\phi_0/2$, both of which are equally favorable energetically. Hence a ring of half magnetic flux quantum is produced with two possible directions, ready for charged particles to interact with. By the AB effect, the single-charged matter wave passing through the ring acquires a phase shift relative to the wave passing outside the ring, receiving essentially zero force unless the wave directly hits the ring. (In Sec. III D, however, we show that the force is, in a certain sense, only exponentially small and hence not zero.) Since we are considering the rf-SQUID *qubit*, we can have a quantum mechanically superposed state of two opposing directions of the magnetic flux ring. The phase acquired by the charged particle, the meaning of which is made precise shortly, depends on the magnetic flux inside the rf-SQUID tube, and the magnetic flux can be in a quantum superposition of two distinct values. Consequently, the charged particle and the rf-SQUID get entangled upon passing of the former through the latter. (A way to utilize such entanglement for electron microscopy has been put forward [5,6].)

We defer to a future study an important aspect of how to realize the magnetic flux ring in practice, while noting that a preliminary consideration has already appeared [6]. It is possible that the eventual implementation of our scheme would involve a superconducting device that is not precisely an rf-SQUID qubit as presented here, for technical reasons that will be discussed briefly in Sec. IV A. However, having a ring of half magnetic flux quantum in the matter wave of a charged particle is an essential part of our scheme.

To study dynamics of rf-SQUID from the electrical circuit perspective, we introduce the inductance of the SQUID loop L, the critical current of the Josephson junction i_0 and the junction capacitance C. As noted earlier, the rf-SQUID loop is biased with a flux $\phi_0/2$. The potential energy of the rf-SQUID is

$$U(\phi) = \frac{\phi^2}{2L} - E_J \cos\left(\frac{2\pi\phi}{\phi_0} + \pi\right), \tag{1}$$

where $E_J = i_0\phi_0/2\pi$ [see Fig. 1(b)] is the Josephson energy. Hence the two qubit states $|0\rangle_q$ and $|1\rangle_q$, respectively associated with the trapped flux $\phi \approx -\phi_0/2$ and $\phi_0/2$, have the same energy. The subscript "q" stands for "qubit" henceforth and all rf-SQUID qubit states will be labeled as such. Dirac's bra-kets without the subscript represent states of the charged particle. For simplicity, we first assume that these values of trapped flux are exactly $\pm\phi_0/2$ and quantum mechanically well defined.

We use a few conventions when studying the device from the electromagnetic perspective. Note that the interaction due to the AB effect remains the same for any single-charged particle, i.e., a particle having a charge $\pm e$, regardless of the species and kinetic energy of the particle (although the sign of charge affects the sign of quantum mechanical phase change). Without loss of generality, throughout the paper we will assume that the charged particle has a negative charge $-e$. We will use the Coulomb gauge $\mathrm{div}\boldsymbol{A} = 0$ for the vector potential $\boldsymbol{A}$ throughout the paper. To make the argument simple and clear, we pretend that the magnetic field $\boldsymbol{B} = \mathrm{rot}\boldsymbol{A}$ only exists in the rf-SQUID tube (much like the discussion of a single point charge at the beginning of an electromagnetism course, where one pretends that there is no other charge in the world). The Coulomb gauge does not completely fix the gauge because we may still have a modification $\boldsymbol{A}' = \boldsymbol{A} + \mathrm{grad}\Lambda$, where the scalar field Λ satisfies $\triangle\Lambda = 0$. This unwanted "freedom" is eliminated by requiring that $\boldsymbol{A}$ goes to zero as the distance from the ring goes to infinity. (This is analogous to a magnetostatic situation, where Ampere's law $\mathrm{rot}\boldsymbol{B} = \mu_0\boldsymbol{j}$, where $\boldsymbol{j}$ is the current density, along with $\mathrm{div}\boldsymbol{B} = 0$, completely determines the $\boldsymbol{B}$ field if we demand that $\boldsymbol{B}$ goes to zero at faraway places.)

The structure of the qubit is intended to shift the phase of a charged particle wave, passing through the hollow ring, by a phase angle $\pm\pi/2$ depending on the qubit state, while not much affecting the phase of the charged particle waves passing outside the ring. To see how this works, first assume that the charged particle with the mass m flies in a region largely without electric or magnetic field and its wave function $\psi(\boldsymbol{r}) = \langle\boldsymbol{r}|\psi\rangle$, where $|\boldsymbol{r}\rangle$ is a position eigenstate normalized

in the standard way, obeys Schrödinger's equation

$$i\hbar\frac{\partial}{\partial t}\psi(\boldsymbol{r}) = \frac{1}{2m}(-i\hbar\nabla + e\boldsymbol{A})^2\psi(\boldsymbol{r}). \quad (2)$$

Note the sign of the term $e\boldsymbol{A}$ because of the negative charge. Note also that, with certain redefinition of the mass and energy values, the "relativistically corrected Schrödinger equation" of the above form can handle relativistic cases typically with good approximation [11]. We assume that the wave function of the charged particle, while certainly localized in some place in charged particle optics in question, can nevertheless be regarded as plane waves $\psi \propto e^{i(\boldsymbol{k}\cdot\boldsymbol{r}-\omega t)}$, where $\boldsymbol{k}$ denotes the wave vector, if we get up close. Then Eq. (2) tells us that

$$2mE = (\hbar\boldsymbol{k} + e\boldsymbol{A})^2, \quad (3)$$

where $E = \hbar\omega$ and we conclude that $\hbar\boldsymbol{k} + e\boldsymbol{A}$ remains constant over the trajectory of the charged particle. On the other hand, Fig. 1(c) shows that the $\boldsymbol{A}$ field is substantial only within the bore of the rf-SQUID, much as a $\boldsymbol{B}$ field would be substantial only in the bore of a solenoid. Incidentally, the state of the $\boldsymbol{B}$ field shown in Fig. 1(c) is defined to correspond to the qubit state $|0\rangle_q$. Since the magnetic flux is half the flux quantum $h/4e$, by Stokes' theorem the line integral of the $\boldsymbol{A}$ field, along the charged particle trajectory going through the rf-SQUID, amounts also to $h/4e$. Hence, if the charged particle goes through the rf-SQUID, $\hbar\boldsymbol{k} + e\boldsymbol{A}$ being constant, in the case of Fig. 1(c) $\boldsymbol{k}$ integrates to a value smaller by $\pi/2$ compared to what would be obtained if the charged particle bypassed the rf-SQUID.

We show that the system comprising the rf-SQUID and a charged particle work as the quantum controlled-NOT (CNOT) gate [12]. Let the quantum state of the matter wave of the charged particle passing through the hollow ring be $|a\rangle = (|0\rangle - |1\rangle)/\sqrt{2}$ and the wave passing outside the ring be $|s\rangle = (|0\rangle + |1\rangle)/\sqrt{2}$, where we also introduced the states $|0\rangle$,$|1\rangle$. (The letters s and a stand for symmetric and antisymmetric, respectively.) By the argument in the preceding paragraph, the charged particle state $|a\rangle$ transforms to $-i|a\rangle$ when the rf-SQUID qubit is in the state $|0\rangle_q$ and likewise the state transforms to $i|a\rangle$ for the qubit state $|1\rangle_q$ with the opposite $\boldsymbol{B}$ field, while the state $|s\rangle$ remains the same. (We assume that there is zero or only a negligible amount of the matter wave component impinging on the body of the hollow ring. This may be done deliberately in certain cases, for example by placing a suitable stencil mask at the upstream of the charged particle beam [6].) Now, consider a process comprising two steps. First, to make it exactly a CNOT gate, the state $|a\rangle$, and not the state $|s\rangle$, receives a phase shift $\pi/2$ and becomes $i|a\rangle$ by a classical charged-particle optical component, which we will call a $\pi/2$ phase shifter [13]. Second, the matter wave passes the rf-SQUID. This whole process flips the sign of the state $|a\rangle$ if and only if the rf-SQUID qubit is in the state $|1\rangle_q$. Hence the process represents the CNOT gate [6], where the rf-SQUID qubit with its logical value represented by the basis states $\{|0\rangle_q,|1\rangle_q\}$ controls the value associated with the charged particle in terms of the basis states $\{|0\rangle,|1\rangle\}$.

Now we are in the position to present one of the main ideas of this paper. The two qubits of any quantum CNOT gate swap their roles of either controlling or being controlled, upon basis change by the Hadamard transform [12]. Let us define symmetric and antisymmetric qubit states $|s\rangle_q = (|0\rangle_q + |1\rangle_q)/\sqrt{2}$ and $|a\rangle_q = (|0\rangle_q - |1\rangle_q)/\sqrt{2}$. In our case, the state of the rf-SQUID qubit in terms of the states $\{|s\rangle_q,|a\rangle_q\}$ is flipped if and only if the matter wave is in the state $|a\rangle$. This immediately suggests a use of the rf-SQUID as a nondestructive charged particle counter, because its quantum state flips if and only if a charged particle flies through it.

We evaluate the above crude idea more quantitatively in the rest of this paper. Let us see more closely how the charged particle in the state $|a\rangle$, flying through the qubit, flips the qubit state. First, let the initial qubit state be $|s\rangle_q$. The initial state of the charged particle is $|a\rangle$, and the $\pi/2$ phase shifter described above may as well be absent because it would change nothing except the overall phase in this particular case of charged particle detection. Thus the initial state of the combined system is

$$|\psi_0\rangle = |a\rangle|s\rangle_q = \frac{|a\rangle|0\rangle_q + |a\rangle|1\rangle_q}{\sqrt{2}}. \quad (4)$$

Upon interaction with the qubit, the charged particle wave follows or goes against the $\boldsymbol{A}$ field, resulting in a phase shift $\pm\pi/2$. The resultant state of the combined system after interaction is

$$\frac{e^{-i\pi/2}|a\rangle|0\rangle_q + e^{i\pi/2}|a\rangle|1\rangle_q}{\sqrt{2}}, \quad (5)$$

which equals, up to an overall phase factor,

$$|\psi_1\rangle = \frac{|a\rangle|0\rangle_q - |a\rangle|1\rangle_q}{\sqrt{2}}. \quad (6)$$

Passing the phase factor to the qubit, the charged particle stays in the initial state, while the qubit state flips as $|\psi_1\rangle = |a\rangle(|0\rangle_q - |1\rangle_q)/\sqrt{2} = |a\rangle|a\rangle_q$.

Now we proceed to the next section, where we examine how actual operations deviate from the above ideal case.

III. EVALUATION OF ERRORS

A. Vector potential outside the rf-SQUID

The first cause of error that we consider with respect to charged particle detection is nonideal $\boldsymbol{A}$ field distribution. Specifically, the difference $\Delta\theta$ between the two phase shifts associated with two qubit states $|0\rangle_q$,$|1\rangle_q$ is generally less than π because of the $\boldsymbol{A}$ field outside the bore of the rf-SQUID. In contrast, the experiment demonstrating the AB effect [14] measures the phase shift difference between two paths, which together encircles the magnetic flux. Writing $\Delta\theta = \pi - \delta$, Eq. (5) is modified to be

$$\frac{e^{-i\frac{(\pi-\delta)}{2}}|a\rangle|0\rangle_q + e^{i\frac{(\pi-\delta)}{2}}|a\rangle|1\rangle_q}{\sqrt{2}} \cong -i|a\rangle|a\rangle_q + \frac{\delta}{2}|a\rangle|s\rangle_q, \quad (7)$$

where higher-order terms in δ are ignored. Hence the error probability for charged particle detection is $\approx \delta^2/4$ if $\delta \ll 1$. To estimate δ, let the length of the inner bore of the rf-SQUID be l and the radius of the bore be $r \ll l$. Let the magnitude of the $\boldsymbol{A}$ field inside the bore be A_{bore}, which we assume to be highly uniform. In other words, just as a good solenoid generates a highly uniform magnetic field $\boldsymbol{B}$ from an electric

current, so does our rf-SQUID generate a highly uniform $\boldsymbol{A}$ field from the magnetic flux. Furthermore, as the operating solenoid may be seen as producing two "magnetic charges" of opposite signs placed at both the ends, the rf-SQUID may be seen as holding a pair of "vector potential charges" (VPCs) $q_A = \pm\pi r^2 A_{\rm bore}$ at the two ends, disregarding the $\boldsymbol{A}$ field inside the bore. Treating these two VPCs as well-separated "point charges," $\boldsymbol{A}$-field distribution outside the rf-SQUID can be computed in the same manner the $\boldsymbol{E}$ field is computed in electrostatics. Specifically, since we disregard the $\boldsymbol{A}$ field inside the bore in this particular consideration, we can define a "potential" φ_A that satisfies $\boldsymbol{A} = -\mathrm{grad}\varphi_A$. In particular, the potential near one of the VPCs, ignoring the influence of another, is given as $\varphi_A \approx q_A/4\pi R$, where R is the distance between the measuring point and the VPC. The potential difference $\Delta\varphi_A$ between the two VPCs would be infinity if these were indeed point charges, but the VPCs have the "size" $\approx r$. Hence the potential difference is approximately $\Delta\varphi_A \approx q_A/2\pi r \approx r A_{\rm bore}/2$, again ignoring the influence of the distant VPC when evaluating the potential at either end of the rf-SQUID. The integral of $\boldsymbol{A}$ along a closed path C interlinking the rf-SQUID once should satisfy

$$\oint_C \boldsymbol{A}\cdot d\boldsymbol{l} \approx A_{\rm bore}\left(l+\frac{r}{2}\right) = \frac{\phi_0}{2}. \tag{8}$$

Since the charged particle flies only inside the bore, the error is $\delta \approx r/2l$. This suggests that an aspect ratio of $l/r \approx 10$ would be sufficient to achieve $\lesssim$1% error or even less for this particular error source. Finally, we remark that the error discussed here does not affect the performance of entanglement-enhanced electron microscopy [5,6], where the phase difference between two paths matter.

B. Shift in the minima of the potential landscape

The second source of phase error is the nonideal amount of magnetic flux inside the rf-SQUID. The separation $\Delta\phi$ between the two potential minima shown in Fig. 1(b) is ideally ϕ_0, but is somewhat less than that. Thus the difference of the phase shift experienced by the flying charged particle in the state $|a\rangle$, with respect to the two states of the rf-SQUID $|0\rangle_q$ and $|1\rangle_q$, is ideally π but is somewhat smaller $\pi-\varepsilon$. Hence we write

$$\pi\Delta\phi/\phi_0 = \pi - \varepsilon. \tag{9}$$

The error probability in terms of charged particle detection is $\approx\varepsilon^2/4$ by the same reasoning used in Sec. III A. On the other hand, the position of the potential minima in Fig. 1(b) equals $\phi = \Delta\phi/2 = (\phi_0/2)(1-\varepsilon/\pi)$. This should satisfy $dU(\phi)/dt = 0$, where $U(\phi)$ is given in Eq. (1). Hence $\pi - \varepsilon = \beta\sin\varepsilon$ follows, where $\beta/2\pi = Li_0/\phi_0$. Numerical calculation reveals that $Li_0 \gtrsim 2.4\phi_0$ should be satisfied to have $\lesssim$1% detection error.

C. Excitation of the qubit state

The flux qubit is not strictly discrete in the sense that spin 1/2 is discrete, and therein lies another source of an error. For example, the wave function $\psi_q(\phi) = {}_q\langle\phi|0\rangle_q$ of the rf-SQUID, where $|\phi\rangle_q$ is an eigenstate of the magnetic flux ϕ, is not fully localized at the potential minimum at $\phi = \pm(1/2-\varepsilon/2\pi)\phi_0$. To see the effect of it, notice a relation $|0\rangle_q = \int\psi_q(\phi)|\phi\rangle_q d\phi$ for the basis system $\{|\phi\rangle_q\}$ normalized as ${}_q\langle\phi|\phi'\rangle_q = \delta(\phi-\phi')$. Since the state $|\phi\rangle_q$ induces a phase shift $\pi\phi/\phi_0$ to the charged particle wave, after interaction with the charged particle the qubit is left in the state $|0'\rangle_q = \int\psi_q(\phi)e^{i\pi\phi/\phi_0}|\phi\rangle_q d\phi$. This state is no longer exactly $|0\rangle_q$, meaning that there is a finite probability $p_l = 1 - |{}_q\langle 0'|0\rangle_q|^2$ that the qubit state is leaked out of its "logical" Hilbert space spanned by $|0\rangle_q$ and $|1\rangle_q$. To estimate the wave-function spread, first use the standard method to obtain the Hamiltonian $H = q^2/2C + \phi^2/2L + E_J\cos(2\pi\phi/\phi_0)$ and the commutation relation $[\phi,q] = i\hbar$. To focus on one of the two potential minima, consider a purely harmonic potential that fits one of the two minima of $U(\phi)$. Differentiating $U(\phi)$ twice, the effective inductance $(d^2U(\phi)/d\phi^2)^{-1}$ at the potential minimum $\phi = (1/2-\varepsilon/2\pi)\phi_0$ is

$$\begin{aligned} L_e &\approx \frac{LL_J}{L(1-\varepsilon^2/2)+L_J} = \frac{\beta}{\beta(1-\varepsilon^2/2)+1}L_J \\ &\approx \frac{\beta}{\beta+1}L_J, \end{aligned} \tag{10}$$

where $L_J = \phi_0/2\pi i_0 = L/\beta$ is the Josephson inductance at zero phase difference across it. Using this, the original Hamiltonian is approximated with a Hamiltonian of a harmonic oscillator, i.e., $H' = q^2/2C + (\phi-\phi_0/2)^2/2L_e$. The ground state is

$$\psi_q(\phi) = \frac{1}{\sqrt[4]{\pi\phi_1^2}}e^{-(\phi-\phi_0/2)^2/2\phi_1^2}, \tag{11}$$

where $\phi_1^2 = \hbar\sqrt{L_e/C}$. Hence we obtain $|{}_q\langle 0'|0\rangle_q|^2$ as

$$\left|\int_{-\infty}^{\infty} d\phi|\psi_q(\phi)|^2\cos\frac{\pi(\phi-\phi_0/2)}{\phi_0}\right|^2 = e^{-\frac{\pi^2}{2}(\frac{\phi_1}{\phi_0})^2} \tag{12}$$

and the leakage probability is $p_l \approx (\pi^2/2)(\phi_1/\phi_0)^2$, or

$$p_l \approx \sqrt{\frac{\beta}{\beta+1}}\sqrt{\frac{E_C}{8E_J}} \tag{13}$$

in terms of E_J and $E_C = e^2/2C$. Assuming $\sqrt{\beta/(\beta+1)} \approx 1$, the ratio E_C/E_J should be $\approx 10^{-3}$ to achieve $\approx$1% detection error, which is not unusual for an rf-SQUID qubit [9].

D. Backaction to the flying charged particle

As discussed earlier, in charged particle detection, the charged particle state $|a\rangle$ is fully disentangled from the rf-SQUID qubit state and remains in the initial state after going through the rf-SQUID. Hence neither spatial nor temporal coherence of the charged particle wave is important. This remarkable robustness suggests that a classical charged particle suffices to explain the device operation. Figure 2(a) shows a cross section of an rf-SQUID, in which a negative charged particle goes through. The rf-SQUID is electrically grounded to a conducting wall with a wire. The charged particle induces the opposite positive charge on the surface of nearby conductors. The positive charge moves along as the charged particle goes through the hollow ring. The reader will

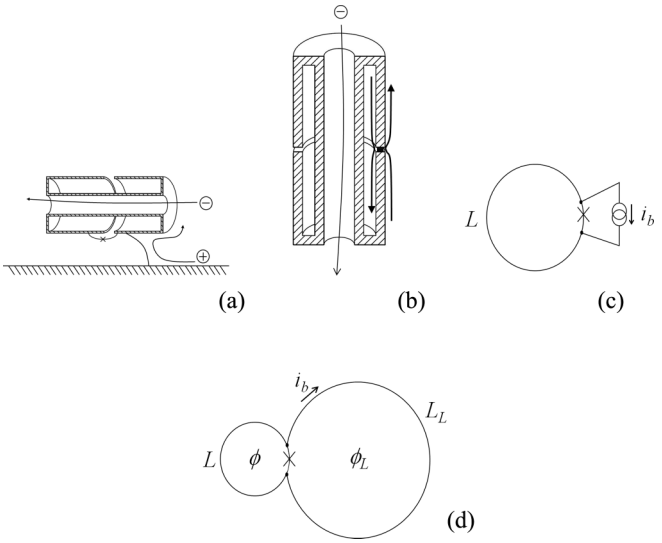

FIG. 2. Nondestructive charge counting operation. (a) Induced positive charge flows on conductor surfaces as the charged particle flies through the rf-SQUID. (b) On a closer inspection, one sees that the current generating the $\boldsymbol{B}$ field inside the rf-SQUID tube and the induced current by the flying charged particle are distinct. For better visibility, the thickness of the superconductor is exaggerated compared to other figures. (c) The flying charged particle is modeled as a current source, which in turn is modeled as another superconducting ring as in (d).

see that a total of charge e will flow through the Josephson junction from left to right, especially when the hollow ring is such that all the electric-field lines from the charged particle terminate on the surface of the rf-SQUID at one point of time during the charged particle's passage. (Here we do not pursue the case of an electrically floating rf-SQUID. While the conducting wire can clearly be replaced by a large capacitor, a full analysis remains to be done.)

Superconducting currents flow only at near the surface of the superconductor, with the current-flowing layer thickness of approximately the London penetration depth (which is $\sim$16 nm for aluminum, the most popular material for superconducting qubits). Since films in typical devices are thicker than this, the current generated by the movement of the induced charge, induced by the flying charged particle, flows on the outer surface of the rf-SQUID comprising finite-thickness superconducting films, whereas the current keeping the magnetic flux inside the hollow ring flows on the inner surface of the device [Fig. 2(b)]. Since these two currents meet essentially only at the Josephson junction, we model the rf-SQUID circuit as in Fig. 2(c), where a current source, producing a current that integrates to e, is attached to near the both sides of the Josephson junction. To make the analysis easier, we replace the current source by a large inductor L_L that traps a large magnetic flux ϕ_L, generating a bias current $i_b = \phi_L/L_L$. We can do this because the rf-SQUID does not "care" about what kind of current source is used. [See Fig. 2(d). This inductor-based current source is only for our thought experiment and need not exist. One is free to imagine changing i_b at will by mechanically deforming the inductor L_L, for example.] Since the total magnetic flux $\phi_t = \phi + \phi_L$, in addition to the bias flux $\phi_0/2$, is firmly trapped within a superconductor, it is a constant. Hence the potential energy of the system is

$$U'(\phi) = \frac{\phi^2}{2L} + \frac{(\phi_t - \phi)^2}{2L_L} - E_J \cos\left(\frac{2\pi\phi}{\phi_0} + \pi\right)$$
$$\approx \frac{\phi^2}{2L} - i_b\phi + E_J \cos\left(\frac{2\pi\phi}{\phi_0}\right) + \text{const}, \qquad (14)$$

where we used $\phi_t \approx \phi_L \gg \phi$ and assumed the absence of mutual inductance between L and L_L. (Incidentally, we found that the bias flux $\phi_0/2$ may be applied by this type of current biasing. However, the required bandwidth of such a bias line may well entail a noise current directly fed to the Josephson junction, especially when the control signal comes from an external circuit.) We set $i_b = e/T$ for a time duration T. Then, one potential minimum goes up by an energy amount $\Delta E = i_b\phi_0/2 = h/4T$, whereas the other minimum goes down by the same amount. As expected, this results in the phase difference $2\Delta ET/\hbar = \pi$ between the states $|0\rangle_q, |1\rangle_q$ because this is the difference in action at least for sudden or adiabatic changes of the potential.

The above argument, although not rigorous, is useful because it provides insights into "backaction" to the charged particle in our device. We consider two mechanisms. The first mechanism is due to the motion of the induced positive charge on the inductive surface of the rf-SQUID. This could influence the motion of the charged particle in essentially a nondissipative way because the induced charge has "inertia" due to the inductance. The dissipative part due to the possible presence of quasiparticles will be considered in the next subsection. This mechanism is generic and a similar effect should be present in any conductor [15].

The second, perhaps more interesting, mechanism transfers energy from the charged particle to the rf-SQUID. First, we make an outline of the argument in physical terms. The charged particle *must* lose energy via some electric field, since the magnetic field would not give or take energy, and the field is inside the rf-SQUID tube anyway. We want to see exactly how the electric field appears. As we have seen in Sec. II, upon passing of the charged particle the state of rf-SQUID changes from the symmetric state $|s\rangle_q$, in which current generating the $\boldsymbol{B}$ field is counterclockwise [$|0\rangle_q$; see Fig. 1(a)] *plus* clockwise ($|1\rangle_q$), to the antisymmetric state $|a\rangle_q$, where the current is counterclockwise *minus* clockwise, both in the sense of macroscopic quantum mechanical superposition. The energy splitting of these two states are proportional to the tunneling frequency with respect to the tunneling process between the two minima [see Fig. 1(b)], and it is this energy that the charged particle should lose. The energy splitting can be exponentially suppressed if the tunneling barrier $U(\phi)$ shown at the center of Fig. 1(b) is modestly increased by controlling the Josephson coupling in the standard manner [16]. This is why we may say that the charged particle receives essentially zero force upon passing the device [17]. As noted above, the reason why the charged particle excites the rf-SQUID is because it induces a current, which "helps" only one of the two superposed clockwise or counterclockwise currents ($|0\rangle_q$ or $|1\rangle_q$), energetically favoring it. This leads to the drift of the relative quantum mechanical phase between the states $|0\rangle_q$

and $|1\rangle_q$, which means the quantum state changes from $|s\rangle_q$ towards $|a\rangle_q$. However, such a change means an appearance of a voltage across the Josephson junction. This is because the existence of the relative phase between the two states $|0\rangle_q$ and $|1\rangle_q$ means the phase change of the wave function $\psi_q(\phi)$ of the rf-SQUID with respect to ϕ. On the other hand, the standard commutation relation $[\phi,q] = i\hbar$ implies that the charge operator can be written as $-i\hbar\partial/\partial\phi$. Hence the "phase change with respect to ϕ" means the appearance of charge across the Josephson junction, which means generation of a voltage. As we will see, this voltage hinders the flow of the current on the outer surface of the rf-SQUID induced by the charged particle, slowing the response of the induced current to the motion of the charged particle, ultimately making the charged particle lose energy. Before proceeding, note that we put aside the possibility of excitation within a single potential well around one of the potential minima, because we have already discussed it in Sec. III C.

Let us examine the above process more closely. Initially, the rf-SQUID is in the state $(|0\rangle_q + |1\rangle_q)/\sqrt{2}$. When the charged particle goes halfway through the rf-SQUID, after factoring out the charged particle state, the state of the rf-SQUID is

$$\frac{e^{-i\delta}|0\rangle_q + e^{i\delta}|1\rangle_q}{\sqrt{2}}, \tag{15}$$

where δ is a small positive real number increasing with time. Although we have essentially seen this in Eq. (5), below we consider this from the perspective centered on energetics of the rf-SQUID. The induced charge motion tends to force magnetic flux, opposite to that generated by the $|0\rangle_q$ state, into the rf-SQUID inductance ring. [See Figs. 1(a) and 2(d). Suppose that the current in the inductor L in Fig. 2(d) flows counterclockwise for the state $|0\rangle_q$ to produce the magnetic flux ϕ, in accordance with the right-hand side of Fig. 1(a). The current i_b in Fig. 2(d) generates a magnetic flux ϕ_L in L_L with the direction opposite to ϕ. Note that i_b does not contribute to ϕ because of the absence of mutual inductance. The finite amount of flux ϕ_L "wants" to go into the loop L unless the inductance L_L is infinitely large.] Arguably, this makes the energy of the $|0\rangle_q$ state higher than that of $|1\rangle_q$, resulting in the phase factor in Eq. (15) because of the $e^{-iEt/\hbar}$ dependence on time. This is valid at least in the following two limits: the energy level actually goes up in the adiabatic approximation, and the potential energy term contributes to the above phase evolution in the sudden approximation.

At some moment the state is $\approx(|0\rangle_q + i|1\rangle_q)/\sqrt{2}$ up to the overall phase factor, which has an associated charge, albeit ill defined, because the charge operator is $q = -i\hbar\partial/\partial\phi$. [Since the phase of the rf-SQUID wave function $\psi_q(\phi)$ rotates mostly within the tunnel barrier, the associated probability amplitude is small when E_J, or the height of the tunnel barrier, is large.] In order to determine the polarity of the Josephson junction charging, assume for the moment the state is exactly

$$\frac{|0\rangle_q + i|1\rangle_q}{\sqrt{2}} \propto \frac{|s\rangle_q - i|a\rangle_q}{\sqrt{2}}, \tag{16}$$

and is freely evolving in the unbiased ($i_b = 0$) potential. Since the state $|a\rangle_q$ has a larger energy than the state $|s\rangle_q$, this state is on the path evolving from $(|s\rangle_q + |a\rangle_q)/\sqrt{2} = |0\rangle_q$ to $(|s\rangle_q - |a\rangle_q)/\sqrt{2} = |1\rangle_q$. From the direction of the current shown in Fig. 1(a) for the state $|0\rangle_q$, we find that the lower electrode of the Josephson junction is positively charged when the state is $(|s\rangle_q - i|a\rangle_q)/\sqrt{2}$. Thus it takes positive work to supply the positive charge to the Josephson junction. This in turn means that the negative charged particle receives a "pulling" force from the positive induced charge, which moves with dissipation on the SQUID surface.

It is possible to make the above argument somewhat more quantitative. The amount of the charge q on the Josephson junction is such that q/C equals the electromotive force, which has the dimension of electrostatic potential, generated by the time-varying magnetic flux inside the SQUID. The oscillation frequency ω between the two states $|0\rangle_q, |1\rangle_q$, which respectively corresponds to the two directions of the magnetic flux, represents the energy splitting $\hbar\omega$ between the states $|s\rangle_q$ and $|a\rangle_q$. On the other hand, the electromotive force is $\sim 2\phi_0\omega/2\pi \sim \hbar\omega/e$. The first factor 2 comes from the fact that the time needed for the flux change ϕ_0 is the half period π/ω. Consequently, as we would expect, the work needed to force the positive charge e across the Josephson junction equals, at least up to a numerical factor, $\hbar\omega$.

As noted before, one may hope to exponentially suppress the energy loss by keeping the tunnel barrier height large. This may be done by dynamically manipulating the effective critical current i_0 of the Josephson junction [18].

E. Excitation of quasiparticles

Various noise sources contribute to the finite qubit coherence time. For instance, even at sufficiently low temperatures nonequilibrium quasiparticles are present in practice, leading to relaxation of a qubit [19]. Although practical matters are important, here we are content to deal only with fundamental matters. While experimentally observed coherence time for superconducting qubits, on the order of μs [20], may be regarded to be already long enough compared to what we need for the one-shot charged particle detection, we have a new situation here, i.e., the passages of the charged particle.

The excitation of quasiparticles by the passage of a charged particle is something we cannot avoid. This is in contrast with quasiparticle excitations due to infrared radiation from the high-temperature parts of the charged particle optics through the entry and exit apertures, because this can in principle be avoided by cooling the entire optics, whether it is practical or not. The problem of excitation by the passing charged particle is especially significant when the charged particle is light, as in the case of the electron, because the light particle tends to move fast. As shown below, a shorter time period leads to more dissipation. For the sake of concreteness, we will talk about electrons in the rest of this subsection.

A fairly rigorous analysis of a flying electron near a superconductor would use the BCS Hamiltonian, with a potential-energy term representing an external time-varying electric field, to see whether quasiparticles are excited. Here we perform a much simpler analysis, whose only purpose is to estimate the order of magnitude. Suppose that the rf-SQUID has the dimension of approximately 100 μm [9]. Since electrons with a sufficiently high energy move approximately

at the speed of light, the time scale τ involved is about 0.3 ps. The energy scale E/τ turns out to be about 20 meV, which is two orders of magnitude greater than the energy gap $\Delta = 180\ \mu$eV of aluminum, the most popular material for the superconducting qubits. Hence we are dealing with an intrinsically high-speed phenomena from the perspective of superconductivity. It is known that energy dissipation in a superconductor due to alternating current is not much different from that in the normal state, provided that the frequency of the alternating current is above Δ/h. Hence we assume that, in our situation, the rf-SQUID behaves like a normal conductor with a resistance R. Roughly, we have the electrical current e/τ, power dissipation $R\,e^2/\tau^2$, energy dissipation $\Delta E = R\,e^2/\tau$, and the change of action $\Delta A = R\,e^2 = (R/R_Q)h$, where $R_Q = h/e^2 = 25.8\,\mathrm{k}\Omega$ is the von Klitzing constant. We would expect $\eta \equiv R/R_Q$ to be small compared to 1. Then, first, quantum coherence is essentially protected because $\Delta A \ll h$. Second, the desired condition that energy dissipation being smaller than the energy gap, namely $\Delta E < \Delta$, is expressed as $\eta h/\tau < \Delta$. It might seem paradoxical that the charged particle travels without quasiparticle excitation, i.e., without energy dissipation, when this inequality is satisfied. A plausible answer is that the dissipation occurs *on average* as we expect. The probability of quasiparticle excitation is considered small if the inequality is satisfied with much leeway, e.g., $\eta < 10^{-3}$. However, exactly how quasiparticles will be excited and how they affect the qubit operation once these are excited are not clear in the above rough estimate. For example, it could be argued that unless a quasiparticle tunnels through the Josephson junction, essentially nothing significant happens. Furthermore, diffusion of quasiparticles could be blocked by the use of a flux transformer. Hence further investigations are warranted.

IV. DISCUSSION

A. Operation sequence of the rf-SQUID

Among many species of superconducting qubits, the rf-SQUID qubit is far from the easiest to control. In particular, when the two qubit states have the difference in trapped flux close to ϕ_0, as is required in our scheme, the typical barrier height is too high to allow for appreciable tunneling probability between the two state. In fact, the experiment that showed the coherence of rf-SQUID qubit [9] employed excited states in each potential well. An alternative strategy is the use of dynamic modulation of the barrier height [18], but its quantum mechanically coherent use has not been experimentally validated. Whether the use of excited states or the dynamic modulation of the barrier height is more advantageous remains to be seen at present. For example, the analysis in Sec. III C needs to be reexamined if we use the excited states.

Another possible avenue for future investigations include the use of multiple superconducting persistent current qubits [21], despite the fact that each of such qubit has quantum states associated with a much smaller magnetic flux compared to ϕ_0. These devices could be combined by the use of a flux transformer. The use of multiple qubits seems a serious possibility now, given recent demonstrations on controlling multiple superconducting qubits [22].

B. Possible application of the charged particle counter

Noninvasive charged particle counting could enable nanoscale assembly of atoms and/or molecules on a substrate, providing these objects can be ionized. The reason is because our scheme is for any single-charged object. Consider an instrument similar to the low-energy electron microscope, to which ions are introduced. The rf-SQUID is placed somewhere in the instrument to count the ions going through it. The density of ions are made sufficiently low that only zero or one ions are counted within a suitable time window. The ion is then decelerated at the objective lens of the low-energy electron microscope, lands on a substrate, and is electrically neutralized. Repeating this at desired locations on the substrate, one would be able to form an array of atoms or molecules in any desired pattern.

In principle, one could envision to apply this scheme to ionized biological molecules because there are ways to produce large ionized biological molecules [23]. This might potentially be a useful tool for synthetic biology because one could immobilize the deposited molecule on a cryogenic substrate during the assembly process. For this idea to succeed, however, the landing energy of the biological molecule should be sufficiently low that the molecule would not be damaged, but at the same time minute charging of the substrate should not significantly affect the trajectory of the molecule.

In actual implementations, keeping the rf-SQUID at the dilution-refrigerator temperature while maintaining electron optical or ion optical access is an issue, since infrared radiation is known to affect superconducting qubit performance [24]. In view of experimental difficulty, however, this scheme does not require coherence of the charged particle waves and hence should be an accessible stepping stone towards realizing entanglement-assisted electron microscopy [5,6].

C. Multiqubit schemes

The above single-qubit charged particle detector scheme can be extended to a multiple-qubit area detector version. Since coherence of the charged particle wave is of particular interest here, we will talk about electrons rather than generic charged particles in this subsection in order to be realistic. We will call the electron optical plane of the array of multiple qubits, or any plane conjugate to it, an image plane. The "far field" with respect to the array, or any plane conjugate to it, will be called a diffraction plane. Because of the linearity of quantum mechanics, the extended scheme allows us to transfer the electron quantum state to a quantum memory as shown below. When combined with a quantum information transfer method for the reverse direction, which will also be discussed below, any multipixel quantum tasks could be performed. A sensible example of such a task is quantum enhanced multiple phase estimation [25] for low-dose electron microscopy.

The multiqubit area detector consists of N rf-SQUIDs. The rf-SQUIDs are bound together to form a two-dimensional array. The array of rf-SQUIDs sharing the ground would presumably be fabricated on a single substrate, to which N holes are drilled appropriately. As shown below, each rf-SQUID qubit must at least be controllable with single qubit gate operations to transfer the quantum state of the electron to the rf-SQUID qubits. Moreover, to transfer quantum data

back to the electron, the N rf-SQUID qubits must be a part of a larger quantum information processor to allow for more complex operations such as coherent CNOT gate operations on some pairs of qubits. In view of today's state of the art in superconducting qubit integration [22], such a quantum information processor may seem a rather remote possibility. However, our purpose here is to know what would be possible if we had such a quantum information processor.

Consider such a two-dimensional array of N rf-SQUIDs, which we label $0,1,\ldots,N-1$. The initial quantum state of all rf-SQUID qubits are $|s\rangle_q$. The state of the rf-SQUID qubit array A, in which only the kth qubit is excited to $|a\rangle_q$, is written as $|k\rangle_A$. Let the electron state going through the kth rf-SQUID qubit be $|k\rangle$, and the initial (unknown) electron state be $\sum_{k=0}^{N-1} c_k|k\rangle$. Because of linearity, after going through the 2D array the state of the system becomes $\sum_{k=0}^{N-1} c_k|k\rangle|k\rangle_A$. The transmitted electron is then detected in the far field with a conventional single-electron area detector. Suppose that the electron is detected in a diffracted state $|D_s\rangle = N^{-1/2}\sum_{k=0}^{N-1} e^{i\theta_k}|k\rangle$, where s is an integer labeling the detection pixel and phases θ_k are known from the electron optical geometry. Let $|D_0\rangle,|D_1\rangle,|D_2\rangle,\ldots$ be orthonormal basis states. Then, the matrix $A_{n,k}$ that satisfies $|D_n\rangle = \sum_{k=0}^{N-1} A_{n,k}|k\rangle$ is unitary. In particular, $A_{s,k} = N^{-1/2}e^{i\theta_k}$. Because of the unitarity, we can also write $|k\rangle = \sum_{n=0}^{N-1} A^*_{n,k}|D_n\rangle$. Since the state before the electron detection can be expanded as

$$\sum_{k=0}^{N-1} c_k|k\rangle|k\rangle_A = \sum_{k=0}^{N-1} c_k A^*_{s,k}|D_s\rangle|k\rangle_A + \sum_{\substack{n=0\\ n\neq s}}^{N-1}\sum_{k=0}^{N-1} c_k A^*_{n,k}|D_n\rangle|k\rangle_A, \quad (17)$$

after the electron is detected in the state $|D_s\rangle$, the 2D detector is left in the state

$$\sum_{k=0}^{N-1} c_k A^*_{s,k}|k\rangle_A \propto \sum_{k=0}^{N-1} c_k e^{-i\theta_k}|k\rangle_A. \quad (18)$$

After suitable single-qubit phase manipulations, one will have transferred the electron quantum state to the rf-SQUID qubit array.

Transferring quantum information back to an electron is more involved and we assume the availability of a quantum computer. The basic idea is to use the qudit-version of quantum teleportation [26]. The quantum state to be transferred to an electron is prepared in a register R of the quantum computer as $\sum_{k=0}^{N-1} d_k|k\rangle_R$. First, an electron is generated in a plane-wave state, which is $N^{-1/2}\sum_{k=0}^{N-1}|k\rangle$. The electron wave then goes through an rf-SQUID qubit array placed on an image plane, which we assume to be one-dimensional for now. After interaction, the state of the electron and the rf-SQUID qubit array is $N^{-1/2}\sum_{k=0}^{N-1}|k\rangle|k\rangle_A$. The next step is to use the quantum computer to perform a Bell measurement on the combined system of the rf-SQUID qubit array and the resister R. (Meanwhile, the electron may have to go through an electron-optical version of a delay line.) Specifically, the state is measured with respect to basis states

$$|\psi_{n,m}\rangle_{AR} = \frac{1}{\sqrt{N}}\sum_{k=0}^{N-1} e^{2\pi i\frac{kn}{N}}|k\rangle_A|(k+m)\mathrm{mod}N\rangle_R, \quad (19)$$

where the range of the labels n and m are $0,1,\ldots,N-1$. It is straightforward to check that these states are orthogonal and hence we can write

$$|\psi_{n,m}\rangle_{AR} = \sum_{k,k'} B_{(n,m),(k,k')}|k\rangle_A|k'\rangle_R, \quad (20)$$

where

$$B_{(n,m),(k,k')} = \frac{\delta_{(k+m)\mathrm{mod}N,k'}e^{2\pi i\frac{kn}{N}}}{\sqrt{N}} \quad (21)$$

is unitary. It follows that

$$|k\rangle_A|k'\rangle_R = \sum_{n,m} B^*_{(n,m),(k,k')}|\psi_{n,m}\rangle_{AR} \quad (22)$$

and the state of the whole system is

$$\frac{1}{\sqrt{N}}\sum_{k,k'} d_{k'}|k\rangle|k\rangle_A|k'\rangle_R = \frac{1}{\sqrt{N}}\sum_{k,k',n,m} d_{k'}B^*_{(n,m),(k,k')}|k\rangle|\psi_{n,m}\rangle_{AR}. \quad (23)$$

If the Bell measurement outcome is (n,m), then the electron state is

$$\sqrt{N}\sum_{k,k'} d_{k'}B^*_{(n,m),(k,k')}|k\rangle = \sum_{k'=0}^{N-1} e^{-2\pi i\frac{(k'-m)n}{N}} d_{k'}|(k'-m)\mathrm{mod}N\rangle, \quad (24)$$

where the overall factor is normalized. Finally, the electron wave is manipulated classically, depending on the outcome (n,m). The phase factors $e^{-2\pi i(k'-m)n/N}$ can be compensated for by applying phase shifts pixelwise at the image plane, using, e.g., a multipixel version of the obstruction-free phase shifter [27]. We obtain

$$\sum_{k=0}^{N-1} d_k|(k-m)\mathrm{mod}N\rangle. \quad (25)$$

Another restoration step $|(k-m)\mathrm{mod}N\rangle \to |k\rangle$ can be carried out similarly by another pixelwise phase shifter on a diffraction plane in the electron optical setup. The states $|k\rangle$ can be expressed as

$$|k\rangle = \frac{1}{\sqrt{N}}\sum_{s=0}^{N-1} e^{2\pi i\frac{ks}{N}}|D_s\rangle, \quad (26)$$

in terms of diffracted states $|D_s\rangle$. Hence the electron state is expressed as

$$\frac{1}{\sqrt{N}}\sum_{k,s} d_k e^{2\pi i\frac{(k-m)s}{N}}|D_s\rangle. \quad (27)$$

To compensate, we apply a phase shift $2\pi ms/N$ to the electron state $|D_s\rangle$. This scheme can be extended to the

two-dimensional case if each pixel is numbered in the raster-scanning manner (see the Appendix). In the latter case, each of the two classical phase shifters, located respectively at an image plane and a diffraction plane, consists of two modified obstruction-free phase-shifting devices oriented orthogonal to each other.

The above scheme is essentially universal in that anything programmable can be done, including generation of entangled electrons [28].

V. CONCLUSION

We studied the rf-SQUID qubit with the hollow-tube-ring geometry, which was originally proposed for improving biological electron microscopy [6]. We found another application, namely charged particle detection that applies essentially no force to the charged particle, in the present work. A possible application of the device to nanofabrication is pointed out. We also identified and evaluated several error sources. These are nonideal vector potential distribution, nonideal places of potential minima, excitations of the qubit state, nonzero backaction to the charged particle, and quasiparticle excitations. We conclude that there is no evidence that any of these error sources is detrimental to the device operation in a significant way. We also investigated how far we could go in principle. It is shown that an area detector comprising many such rf-SQUID qubits could in principle be used to transfer quantum information between the charged particle and a quantum information processor, in both the directions.

More work needs to be done, besides the obvious need for experimental studies. In particular, it remains to be seen whether dynamic modulation of Josephson barrier height is a viable strategy, or rather some other circuit topology needs to be explored.

ACKNOWLEDGMENT

This research was supported in part by the Japan Society for the Promotion of Science Kakenhi (Grant No. 25390083).

APPENDIX: CASE OF A TWO-DIMENSIONAL rf-SQUID QUBIT ARRAY

Here we spell out steps for quantum information transfer from the two-dimensional rf-SQUID qubit array to an electron.

We assume that the rf-SQUIDs are on a square lattice on the xy plane, which is perpendicular to the optical z axis. Let the number of rf-SQUIDs along the x and y axes be respectively N_x and N_y, so that the total number of rf-SQUID is $N = N_x N_y$. Each rf-SQUID has a label (k_x,k_y) comprising two integers, with the range $0 \leqslant k_x < N_x$ and $0 \leqslant k_y < N_y$. These two integers k_x,k_y respectively specify the position of the rf-SQUID along the x and y axes. Next, we define a single-integer label $k \equiv k_x + N_x k_y$, which range from 0 to $N-1$. With this label, the argument in the main text goes through without modification also in the present two-dimensional case.

However, it may be useful to elaborate on the final classical electron-wave manipulation step. Let us write $k' = (k-m) \bmod N$. The electron state before the final step is

$$\sum_{k=0}^{N-1} e^{-2\pi i \frac{(k-m)n}{N}} d_k |(k-m) \bmod N\rangle = \sum_{k'=0}^{N-1} e^{-2\pi i \frac{k'n}{N}} d_k |k'\rangle. \tag{A1}$$

Note that $d_k = d_{(k'+m) \bmod N}$. This can be written as

$$\sum_{k'=0}^{N-1} e^{-2\pi i \frac{n}{N} k'_x} e^{-2\pi i \frac{n}{N_y} k'_y} d_k |k'\rangle. \tag{A2}$$

Hence the experimenter can first apply a phase shift $2\pi n k'_x/N$ to the k'_xth row, and then another phase shift $2\pi n k'_y/N_y$ to the k'_yth column to obtain

$$\sum_{k'=0}^{N-1} d_k |k'\rangle. \tag{A3}$$

In terms of instrumentation, the first phase shift can be applied with the multipixel version of the obstruction-free phase shifter [27] oriented along the x axis, and the second phase shift can likewise be applied by another one aligned with the y axis.

To further correct the above state, transformation $|k'\rangle \to |k\rangle$ is carried out. To do so, we need to go to the Fourier space. This is done naturally in electron optics, as one can use a lens system to obtain the far-field wave function. Let us label the pixels in the far field with integers $s = 0,1,2,\ldots,N-1$ and write the diffracted electron state going to the sth pixel $|D_s\rangle$. Following the numbering method used in the image plane, we write $s = s_x + N_x s_y$, and also $m = m_x + N_x m_y$. Since the transformation between $|k'\rangle$ and $|D_s\rangle$ is essentially the two-dimensional Fourier transform, we write

$$|k'\rangle = \frac{1}{\sqrt{N}} \sum_{s_x=0}^{N_x-1} \sum_{s_y=0}^{N_y-1} e^{2\pi i \frac{k'_x s_x}{N_x}} e^{2\pi i \frac{k'_y s_y}{N_y}} |D_s\rangle. \tag{A4}$$

Analogous to the image-plane case, the experimenter can first apply a phase shift $2\pi m_x s_x/N_x$ to the s_xth row, and then another phase shift $2\pi m_y s_y/N_y$ to the s_yth column in the diffraction plane to obtain $|k\rangle$ back in the image plane. Because of the principle of superposition, this means that the above state $\sum_{k'=0}^{N-1} d_k |k'\rangle$ transforms to $\sum_{k=0}^{N-1} d_k |k\rangle$, which is what we wanted.

[1] H.-J. Briegel, W. Dur, J. I. Cirac, and P. Zoller, Phys. Rev. Lett. **81**, 5932 (1998).

[2] C. Monroe, R. Raussendorf, A. Ruthven, K. R. Brown, P. Maunz, L. M. Duan, and J. Kim, Phys. Rev. A **89**, 022317 (2014).

[3] B. B. Blinov, D. L. Moehring, L.-M. Duan, and C. Monroe, Nature (London) **428**, 153 (2004).

[4] M. H. Devoret and R. J. Schoelkopf, Science **339**, 1169 (2013).

[5] H. Okamoto, Phys. Rev. A **85**, 043810 (2012).

[6] H. Okamoto and Y. Nagatani, Appl. Phys. Lett. **104**, 062604 (2014).

[7] R. Henderson, Q. Rev. Biophys. **28**, 171 (1995).

[8] N. Daniilidis, D. J. Gorman, L. Tian, and H. Haffner, New J. Phys. **15**, 073017 (2013).
[9] J. R. Friedman, V. Patel, W. Chen, S. K. Tolpygo, and J. E. Lukens, Nature (London) **406**, 43 (2000).
[10] W. Ehrenberg and R. E. Siday, Proc. Phys. Soc. B **62**, 8 (1949); Y. Aharonov and D. Bohm, Phys. Rev. **115**, 485 (1959).
[11] A. Rother and K. Scheerschmidt, Ultramicroscopy **109**, 154 (2009).
[12] M. A. Nielsen and I. L. Chuang, *Quantum Computation and Quantum Information* (Cambridge University Press, Cambridge, UK, 2000).
[13] R. Danev and K. Nagayama, Ultramicroscopy **88**, 243 (2001); R. Cambie, K. H. Downing, D. Typke, R. M. Glaeser, and J. Jin, *ibid.* **107**, 329 (2007).
[14] A. Tonomura, N. Osakabe, T. Matsuda, T. Kawasaki, J. Endo, S. Yano, and H. Yamada, Phys. Rev. Lett. **56**, 792 (1986).
[15] For the case of a dissipative normal conductor, see P. Sonnentag and F. Hasselbach, Phys. Rev. Lett. **98**, 200402 (2007).
[16] Typically, the single Josephson junction is replaced by two Josephson junctions in parallel. A magnetic flux between these junctions controls the "effective Josephson energy" of the whole system seen as a single Josephson junction.
[17] Indeed, even when the tunneling frequency was on the order of ∼100 GHz, which roughly corresponds to the energy gap of aluminum (and hence the largest possible), the energy splitting would still be less than 1 meV.
[18] S. Poletto, F. Chiarello, M. G. Castellano, J. Lisenfeld, A. Lukashenko, C. Cosmelli, G. Torrioli, P. Carelli, and A. V. Ustinov, New J. Phys. **11**, 013009 (2009).
[19] G. Catelani, J. Koch, L. Frunzio, R. J. Schoelkopf, M. H. Devoret, and L. I. Glazman, Phys. Rev. Lett. **106**, 077002 (2011).
[20] A. Blais, R.-S. Huang, A. Wallraff, S. M. Girvin, and R. J. Schoelkopf, Phys. Rev. A **69**, 062320 (2004).
[21] J. E. Mooij, T. P. Orlando, L. Levitov, L. Tian, C. H. van der Wal, and S. Lloyd, Science **285**, 1036 (1999).
[22] R. Barends, J. Kelly, A. Megrant, A. Veitia, D. Sank, E. Jeffrey, T. C. White, J. Mutus, A. G. Fowler, B. Campbell, Y. Chen, Z. Chen, B. Chiaro, A. Dunsworth, C. Neill, P. O'Malley, P. Roushan, A. Vainsencher, J. Wenner, A. N. Korotkov, A. N. Cleland, and J. M. Martinis, Nature (London) **508**, 500 (2014).
[23] S. J. Gaskell, J. Mass Spectrom. **32**, 677 (1997); L. F. Marvin, M. A. Roberts, and L. B. Fay, Clin. Chim. Acta **337**, 11 (2003).
[24] R. Barends, J. Wenner, M. Lenander, Y. Chen, R. C. Bialczak, J. Kelly, E. Lucero, P. O'Malley, M. Mariantoni, D. Sank, H. Wang, T. C. White, Y. Yin, J. Zhao, A. N. Cleland, J. M. Martinis, and J. J. A. Baselmans, Appl. Phys. Lett. **99**, 113507 (2011).
[25] P. C. Humphreys, M. Barbieri, A. Datta, and I. A. Walmsley, Phys. Rev. Lett. **111**, 070403 (2013).
[26] C. H. Bennett, G. Brassard, C. Crepeau, R. Jozsa, A. Peres, and W. K. Wootters, Phys. Rev. Lett. **70**, 1895 (1993).
[27] H. Rose, Philos. Trans. R. Soc. A **367**, 3809 (2009).
[28] In a sense, any set of identical fermions are entangled because of antisymmetrization of the wave function. Needless to say, this is not what is meant here.